As for the cation, the two open-chain species have equal stability. Thus we will also make an analysis of the isomerization process E ⇄ D through a rotation about the P–C bond. The transition state for this process corresponds to a structure with the PCPH dihedral angle of 90° in which the two P–C bonds have quite different lengths (Figure 12). The barrier is lower compared to the case of cations but still quite important (93.5 kJ·mol$^{-1}$). Since an increase of this barrier is expected in the case of substituted derivatives, experimental observation of the isomerization is very unlikely.

From the above discussion, a mechanism can be proposed for the anionic ring opening of diphosphirane: the cyclic anion undergoes a conrotatory process with a low barrier to a much more stable open form. Taking into account the molecular geometry constraints, we believe that the substituted derivatives allow only an exo–exo conformation.

These results are in good agreement with experimental observations. We found that the reaction of organolithium with symmetric monohalogenated diphosphiranes is stereoselective. Our calculation corroborate the exo–exo structure of the allyl intermediate, identified experimentally at low temperature.

## Conclusion

Throughout this study we have specified the characteristics of the addition mechanism of singlet carbene to diphosphene. The preferential process corresponds to a $\pi$ addition leading to the most stable structure, the diphosphirane.

In agreement with the experimentally observed isomerization, the most stable product of P–P bond rupture appears to be the 1,3-diphosphapropene.

The cationic and anionic ring-opening processes of diphosphirane were examined. In the case of cations there is no potential energy barrier toward P–P bond rupture which leads directly to exo–endo open-chain species through a disrotatory process. In the case of anions, the ring opening process goes through a cyclic anionic intermediate and then leads to exo–exo open-chain species through a conrotatory process.

Our results are in good agreement with the recently published study of Liu and Bachrach,[18] who examined the possible formation of 1,3-diphosphaallene from the lithio supersystem.

**Acknowledgment.** We thank the Direction Chimie du CNRS for the calculation time allocation on the VP 200 computer of the CIRCE and the GRECO Basses coordinences.

**Registry No.** $CH_2$, 2465-56-7; HP=PH, 41916-72-7; $\overline{CH{=}P{-}PH{\cdot}H^+}$, 140390-35-8; HP=CH—P$^+$H, 102146-41-8; $\overline{HC^-{-}Ph{-}PH}$, 140390-36-9; HP=CH—P$^-$H, 140390-37-0; diphosphirane, 66272-09-1; methylenediphosphene, 140390-33-6; *cis*-diphosphapropene, 133349-80-1; *trans*-diphosphapropene, 133349-79-8; methylphosphinophosphinidene, 140390-34-7.

Contribution from the Dipartimento di Chimica Inorganica, Chimica Fisica e Chimica dei Materiali dell'Università di Torino, Via P. Giuria 7, 10125 Turin, Italy, Dipartimento di Chimica dell'Università di Firenze, Via Maragliano 76/77, 50144 Florence, Italy, and Bracco SpA, Via E. Folli 50, Milan, Italy

# Synthesis, Characterization, and $1/T_1$ NMRD Profiles of Gadolinium(III) Complexes of Monoamide Derivatives of DOTA-like Ligands. X-ray Structure of the 10-[2-[[2-Hydroxy-1-(hydroxymethyl)ethyl]amino]-1-[(phenylmethoxy)methyl]-2-oxoethyl]-1,4,7,10-tetraazacyclododecane-1,4,7-triacetic Acid–Gadolinium(III) Complex

Silvio Aime,*,† Pier Lucio Anelli,‡ Mauro Botta,† Franco Fedeli,‡ Maurizio Grandi,‡ Paola Paoli,§ and Fulvio Uggeri‡

*Received September 16, 1991*

The synthesis of two novel DOTA-like ligands (**5a,b**) containing a polyhydroxy(benzyloxy)propionamide substituent and their Gd(III) complexes (**6a,b**) is reported. Debenzylation by hydrogenolysis of the latter complexes in the presence of Pd/C leads to the corresponding derivatives (**7a,b**) with a primary alcoholic function. Water proton relaxation rates of aqueous solutions of **6a,b** and **7a,b** strongly suggest that these complexes contain only one water molecule in their inner coordination sphere, as was previously found for the parent DOTA complex. The high formation constants measured for complexes **6a,b** (log $K_{ML}$ = 25.9 and 26.4, respectively) support the hypothesis of a direct involvement of the amide functionality in the coordination cage. This was shown by the determination of the solid-state structure of **6a**, which was accomplished in a single-crystal X-ray diffraction study. The structure consists of a $Gd(C_{27}H_{40}N_5O_{10})(H_2O)$ unit and three water molecules; space group $P2_1/c$ ($Z$ = 4) with $a$ = 17.378 (4) Å, $b$ = 8.283 (7) Å, $c$ = 22.813 (5) Å, $\beta$ = 100.33 (2)°, $V$ = 3230 (3) Å$^3$, $d$ = 1.590 g/mL. The coordination polyhedron around the gadolinium ion is best described by a distorted-square antiprism capped by the coordinated water oxygen. All Gd–O distances (ranging from 2.34 to 2.43 Å) are very similar and this unambiguously proves the coordination of the carboxamide oxygen to the gadolinium ion. The $1/T_1$ NMRD profiles of aqueous solutions of **6a,b** and **7a,b** reveal that at the higher frequencies, the solvent proton relaxation rates are dominated by the molecular reorientational time $\tau_R$; i.e., the observed relaxivities are linearly related to the molecular size. However, the main effect associated with the transformation of carboxylate to carboxamide is the drastic reduction of the electronic relaxation time $\tau_{SO}$, which is responsible for a decrease in relaxivity at the low fields.

## Introduction

In recent years, magnetic resonance imaging (MRI) has been recognized as a powerful diagnostic tool in clinical practice.[1] The images (mainly due to the NMR signal of water protons) are the result of the complex interplay between a number of parameters, such as proton density, flow, and $T_1$ and $T_2$ relaxation times. An improvement in the contrast may be achieved by the administration of exogenous chemicals that significantly alter the NMR properties of water resonance.[2,3] Paramagnetic gadolinium complexes, owing to their capability of decreasing the relaxation time of nearby nuclei via dipolar interaction, are under intense scrutiny,[2,3] and a few of them are already in clinical use as contrast agents for MRI.[4]

† Università di Torino.
‡ Bracco SpA.
§ Università di Firenze.

(1) For extensive references, cf.: Stark, D. D., Bradley, W. G., Jr., Eds. "Magnetic Resonance Imaging" The C.V. Mosby Company, St. Louis, Missouri (USA), 1988.
(2) Lauffer, R. B. *Chem. Rev.* **1987**, *87*, 901.
(3) Koenig, S. H. *Isr. J. Chem.* **1988**, *28*, 345.
(4) Gd-DTPA, diethylenetriaminepentaacetic acid gadolinium complex di-*N*-methylglucamine salt, MAGNEVIST, Schering; Gd-DOTA, 1,4,7,10-Tetraazacyclododecane-*N*,*N'*,*N''*,*N'''*-tetraacetic acid gadolinium complex *N*-methylglucamine salt, DOTAREM, Guerbet.

0020-1669/92/1331-2422$03.00/0 

For this purpose, the choice of the proper compound is based on the evaluation of several parameters such as water proton relaxivity, toxicity, body distribution, etc. Basically, two properties are required for a Gd(III) complex to be considered a potential contrast agent in MRI: (i) high thermodynamic (and possibly kinetic) stability; (ii) presence of at least one water molecule in the inner coordination sphere. On the basis of its higher thermodynamic and kinetic stability, Gd–DOTA[5] is currently preferred to Gd–DTPA,[6] the first compound used as an MRI contrast agent.

The water proton relaxation enhancement induced by these paramagnetic chelates can be increased by conjugating them to macromolecules, such as albumin. This is achieved via the formation of an amide bond between an acetate group of the complex and an amino group of the macromolecule.[7,8]

However, passing from carboxylate to amide functionality alters the particular geometry of these ligands, which may decrease the stability of their Gd chelates.

In this paper, we deal with the synthesis and characterization of new Gd(III) complexes of amide derivatives of DOTA-like ligands and with the evaluation of the physicochemical properties that are relevant to a potential application of the compounds as contrast agents in MRI.

## Experimental Section

Preparative HPLC purifications were performed on a Waters preparatory LC/SYSTEM 500A liquid chromatograph. Electrodialyses were carried out with a Hydro Air Research ED-0.4 instrument fitted with seven cation- and five anion-exchange STX membranes (total exchange surface: 0.33 $m^2$). $^1H$ and $^{13}C$ NMR spectra were recorded on a Bruker AC 200 spectrometer. The $^1H$ NMR spectra of **3b**, **4a**, and **5a,b** are not reported because they are not useful for the assignment of structures due to the broadness and extreme overlapping of the signals. The $^{13}C$ NMR spectra of compounds **3b**, **4b**, and **5b**, recorded at room temperature, showed the presence of two conformational isomers due to the presence of the tertiary amide group; the chemical shifts accounting for the minor isomer are quoted in parentheses. Satisfactory elemental analyses (±0.4% for C, H, N, Cl, and Gd) were obtained for all new compounds.

Organic and inorganic reagents were purchased from E. Merck, Darmstadt, Germany, and used without further purification. 2-Chloro-3-(phenylmethoxy)propanoic acid,[9] 1,4,7,10-tetraazacyclododecane,[10] and the Gd–DOTA complex[11] were prepared according to known procedures.

**(*R*)- and (*S*)-2-Chloro-3-(phenylmethoxy)propanoic Acid [(*R*)- and (*S*)-1].** (*R*)-(1-Phenylethyl)amine (327 g, 2.7 mol) was slowly added to a stirred solution of 2-chloro-3-(phenylmethoxy)propanoic acid (578 g, 2.7 mol) in $Et_2O$ (3.9 L) at 25 °C. After filtration of the resulting suspension, the solid residue was crystallized twice from $H_2O$ yielding (*R*)-(1-phenylethyl)ammonium (*R*)-2-chloro-3-(phenylmethoxy)-propanoate (352.8 g; 78%): mp 122 °C; $[\alpha]^{20}_D = +14.3°$ (*c* 5.027, MeOH). The combined ethereal solution and the crystallization mother liquors were acidified with concentrated HCl (250 mL). The organic layer was washed with $H_2O$ (500 mL), dried ($Na_2SO_4$), and diluted with $Et_2O$ (1 L). Slow addition of (*S*)-(1-phenylethyl)amine (182 g, 1.5 mol) gave a white precipitate, which was filtered and crystallized twice ($H_2O$), thus yielding (*S*)-(1-phenylethyl)ammonium (*S*)-2-chloro-3-(phenylmethoxy)propanoate (355.0 g; 78%): mp 123 °C $[\alpha]^{20}_D = -14.0°$ (*c* 5.012, MeOH). Acids (*R*)-**1** and (*S*)-**1** were obtained as viscous liquids from the corresponding salts by the usual procedure.

(*R*)-**1**: $[\alpha]^{20}_D = -2.13°$, $[\alpha]^{20}_{577} = -2.25°$, $[\alpha]^{20}_{546} = -2.48$, $[\alpha]^{20}_{436} = -4.18$ (*c* 5.001 MeCN); $^1H$ NMR ($CDCl_3$) δ 3.92 (dd, 1 H), 3.95 (dd, 1 H), 4.53 (dd, 1 H), 4.65 (bs, 2 H), 7.40 (bs, 5 H); $^{13}C$ NMR ($CDCl_3$) δ 50.7, 70.7, 73.6, 127.9, 128.1, 128.6, 136.9, 173.4.

(*S*)-**1**: $[\alpha]^{20}_D = +2.10°$, $[\alpha]^{20}_{577} = +2.21°$, $[\alpha]^{20}_{546} = +2.48$, $[\alpha]^{20}_{436} = +4.20$ (*c* 5.014, MeCN). Acids (*R*)-**1** and (*S*)-**1** obtained by this method were >98% optically pure. Optical purity was determined by HPLC analysis after derivatization with (*S*)-2-octanol.

**Determination of the Configuration of (*R*)-1.** Optically pure 2-chloro-3-(phenylmethoxy)propanoic acid (10.7 g, 0.05 mol), which had been obtained from the salt precipitated with *R*-1-(phenylethyl)amine, was dissolved in 15 N aqueous $NH_4OH$ (200 mL), and the resulting solution was stirred at room temperature for 28 days. After workup *O*-benzylserine having $[\alpha]^{20}_D = +7.27°$ (*c* 5.00, 1 N HCl) was recovered and compared with an analytical standard of (*S*)-*O*-benzylserine ($[\alpha]^{20}_D = +7.32°$). Considering the pure $S_N2$ mechanism for the aminolysis reaction, the *R* configuration was assigned to the starting chloro acid.

**2-Chloro-3-(phenylmethoxy)propanoyl Chloride (2).** A solution of acid **1a** (107.3 g, 0.5 mol) in thionyl chloride (152 g, 1.28 mol) was refluxed for 2.5 h. After removal in vacuo (15 mbar) of the excess thionyl chloride, distillation of the residue yielded **2** as a colorless liquid (95.8 g, 82%): bp 125–131 °C (0.05 mbar); $^1H$ NMR ($CDCl_3$) δ 3.89 (d, 1 H), 3.91 (d, 1 H), 4.6 (s, 2 H), 4.7 (t, 1 H), 7.3 (m, 5 H); $^{13}C$ NMR ($CDCl_3$) δ 62.5, 70.4, 73.8, 127.8, 128.1, 128.5, 136.7, 169.0.

**(*R*)-2-Chloro-3-(phenylmethoxy)propanoyl chloride [(*R*)-2]** was prepared from (*R*)-**1** as described for **2**, in 92% yield; $[\alpha]^{20}_D = -9.31°$ (*c* 5.022, MeCN).

***N*-[2-Hydroxy-1-(hydroxymethyl)ethyl]-2-chloro-3-(phenylmethoxy)-propanamide (3a).** A solution of **2** (70 g, 0.3 mol) in THF (150 mL) was added in 2 h to a solution of 2-amino-1,3-propanediol (32.6 g, 0.36 mol) in THF/$H_2O$ (5:3, v/v; 400 mL). During the addition the temperature was maintained at 18–20 °C by a cooling bath and the pH at 10 by addition of 6 N NaOH (46.2 mL). After 30 min, $H_2O$ (250 mL) was added and THF removed in vacuo. The resulting aqueous suspension was filtered; the solid was washed with $H_2O$ (2 × 200 mL) and crystallized from $H_2O$ to give **3a** (62.6 g; 72%) as a white solid: mp 133–135 °C; $^1H$ NMR (DMSO-$d_6$) δ 3.4 (m, 4 H), 3.6–3.7 (m, 1 H), 4.5 (s, 2 H), 4.7 (m, 1 H), 7.3 (s, 5 H), 8.05 (d, 1 H); $^{13}C$ NMR (DMSO-$d_6$) δ 53.2, 56.2, 59.7, 70.9, 72.2, 127.6, 128.3, 137.9, 166.6.

**(*R*)-1-[[2-Chloro-3-(phenylmethoxy)-1-oxopropyl]methylamino]-1-deoxy-D-glucitol (3b)** was prepared from (*R*)-**2** and D-*N*-methylglucamine as described for **3a**. The crude product was first run through an Amberlite IR 120 ($H^+$ form) cation-exchange resin and a Duolite A30B ($OH^-$ form) anion-exchange resin and then crystallized twice from EtOAc (yield 48%). **3b**: white solid, mp 98 °C; $[\alpha]^{20}_D = -21.79°$ (*c* 5.046, MeOH); $^{13}C$ NMR (MeOD) δ 35.1 (33.0), 53.1, 54.5 (53.5), 67.9, 76.0 (75.9), 77.4 (77.1), 78.0, 79.1, 79.7, 79.9, 146.2, 146.9, 158.6, 196.9 (196.5).

**1-[1-[(Phenylmethoxy)methyl]-2-[[2-hydroxy-1-(hydroxymethyl)-ethyl]amino]-2-oxoethyl]-1,4,7,10-tetraazacyclododecane (4a).** A solution of 1,4,7,10-tetraazacyclododecane (34.4 g, 0.2 mol) and **3a** (172.6 g, 0.6 mol) in dimethylformamide (DMF) (180 mL) was stirred at 50 °C for 50 h. The reaction mixture was poured into $H_2O$ (1200 mL), and the resulting precipitate (unreacted **3a**) was filtered out and washed with $H_2O$. The combined aqueous solutions were concentrated to a syrup (130 g), which was dissolved in $H_2O$, acidified (pH 1) with concentrated HCl (80 mL), and continuously extracted with $CH_2Cl_2$ until the aqueous layer contained only **4a** and 1,4,7,10-tetraazacyclododecane (TLC). To the aqueous solution was added 5 N NaOH (190 mL), and the solution thus obtained was extracted with $CH_2Cl_2$ (3 × 700 mL). The combined organic solutions were washed with $H_2O$ (3 × 100 mL), dried, and evaporated. The residue was dissolved in EtOH (200 mL) and acidified with 6 N HCl in EtOH (100 mL). The resulting white precipitate was filtered out and crystallized from 96% EtOH (1200 mL) to give **4a**·3HCl (50.1 g; 47%) as a white solid: mp 193–199 °C dec; $^{13}C$ NMR ($D_2O$) δ 43.8, 45.0, 47.0, 47.6, 55.6, 62.4, 63.1, 69.0, 76.2, 131.7, 131.8, 139.8, 173.5. A solution of **4a**·3HCl in $H_2O$ was treated with 3 mol equiv of NaOH and then extracted with $CH_2Cl_2$. After evaporation of the organic phase, crystallization of the residue from EtOH gave **4a** as a white solid: mp 147 °C; $^{13}C$ NMR ($D_2O$) δ 46.4, 47.9, 50.6, 55.3, 63.0, 64.6, 70.1, 75.5, 130.9, 131.3, 140.1, 175.3.

**(*S*)-1-[[3-(Phenylmethoxy)-2-(1,4,7,10-tetraazacyclododec-1-yl)-1-oxopropyl]methylamino]-1-deoxy-D-glucitol (4b).** A mixture of 1,4,7,10-tetraazacyclododecane (17.2 g, 0.1 mol) and **3b** (39.1 g, 0.1 mol) was stirred at 80 °C for 4 h. The crude reaction mixture was cooled to room temperature and dissolved in $H_2O$ (200 mL). After acidification (pH 2) with phosphoric acid, the solution was concentrated to half the volume and purified by preparative HPLC [PrepPAK Prep $C_{18}$/125-Å (55–105-μm) column; 0.001 M aqueous $H_3PO_4$]. The product-containing fractions were combined and passed through an Amberlite A30B ($OH^-$ form) anion-exchange resin. Evaporation of the aqueous solution and drying of the residue ($P_2O_5$; 50 °C; 1 mbar) yielded **4b** (24.4; 46%) as a white solid: mp 68–69 °C; $[\alpha]^{20}_D = -33.9°$ (*c* 5.002, EtOH); $^{13}C$ NMR ($D_2O$) δ 39.6 (36.3), 46.6, 46.7, 48.1, 48.2, 51.2, 51.3, 53.8, 55.3, 61.4 (61.3), 65.5 (65.4), 69.17, 72.0, 72.6, 73.0, 73.7, 74.3, 75.7 (75.6), 131.0, 131.3, 140.1, 176.0 (175.8).

**10-[2-[[2-Hydroxy-1-(hydroxymethyl)ethyl]amino]-1-[(phenylmethoxy)methyl]-2-oxoethyl]-1,4,7,10-tetraazacyclododecane-1,4,7-triacetic**

(5) Geraldes, C. F. G. C.; Sherry, A. D.; Brown, R. D., III; Koenig, S. H. *Magn. Reson. Med.* **1986**, *3*, 242.
(6) Gries, H.; Miklautz, H. *Physiol. Chem. Phys. Med. NMR* **1984**, *16*, 105.
(7) Lauffer, R. B.; Brady, T. J. *Magn. Reson. Imaging* **1985**, *3*, 11.
(8) Ogan, M. D.; Schmiedl, U.; Mosely, M. E.; Grood, W.; Paajanen, H.; Brasch, R. C. *Invest. Radiol.* **1987**, *22*, 665.
(9) Grassman, W. *Chem. Ber.* **1958**, *91*, 538.
(10) Richman, J. E.; Atkins, I. J. *J. Am. Chem. Soc.* **1974**, *96*, 2268.
(11) Desreaux, J. F. *Inorg. Chem.* **1980**, *19*, 1319.

**Acid (5a).** To a stirred solution of bromoacetic acid (200 g, 1.44 mol) in $H_2O$ (700 mL), which was maintained at −5–0 °C, 5 N NaOH was added until the pH was adjusted to 5.0. After addition of **4a**·3HCl (178 g, 0.334 mol), the suspension was stirred at −5–0 °C, and the pH was adjusted to 10 by addition of 5 N NaOH. The resulting solution was slowly (2 h) heated to 50 °C and kept at that temperature for 15 h. The pH was maintained at 10 by continuous addition of 5 N NaOH. After cooling to room temperature and dilution with $H_2O$ (1 L), the reaction mixture was passed through an Amberlite IR 120 ($H^+$ form) cation-exchange resin. Crystallization of the crude product from $H_2O$ gave **5a** (164 g; 82%) as a white solid: mp 138 °C; $^{13}C$ NMR ($D_2O$) δ 48.0, 48.8, 49.9, 51.2, 53.1, 53.8, 53.9, 54.7, 55.3, 55.9, 59.3, 61.9, 63.0, 63.1, 71.6, 76.0, 131.1, 131.2, 131.5, 140.0, 172.2, 172.6, 174.6, 177.1.

**(*S*)-1-[[3-(Phenylmethoxy)-2-[4,7,10-tris(carboxymethyl)-1,4,7,10-tetraazacyclododec-1-yl]-1-oxopropyl]methylamino]-1-deoxy-D-glucitol (5b).** A solution of **4b** (23.1 g, 0.0438 mol) in $H_2O$ (60 mL) was dropped in 2 h into a stirred solution of bromoacetic acid (24.3 g, 0.175 mol) in $H_2O$ (25 mL), which was maintained at 10 °C. The pH was adjusted to 10 by adding 5 N NaOH, and the reaction mixture was heated to 50 °C and kept at that temperature for 2 h. The pH was maintained at 10 by continuous addition of 5 N NaOH. After cooling to room temperature and dilution with $H_2O$ (500 mL), the reaction mixture was passed through an Amberlite IR 120 ($H^+$ form) cation-exchange resin. The crude product was recovered from the resin eluting with 2.5 N aqueous ammonia. The residue obtained after evaporation of the solution was dissolved in $H_2O$ (60 mL). After acidification at pH 3 with phosphoric acid, the solution was purified by HPLC [Lichroprep RP 8 (40–63-μm) column; 0.001 M aqueous $H_3PO_4$:MeCN = 20:1 (v/v)]. The product-containing fractions were combined, concentrated (2 L), and desalted by electrodialysis. The resulting solution was evaporated in vacuo, and the residue was dried ($P_2O_5$; 50 °C; 1 mbar) to give **5b** (14.2 g; 46%) as a white solid: mp 139–141 °C; $[\alpha]^{20}_D$ = −94.5° (*c* 5.062, $H_2O$); $^{13}C$ NMR ($D_2O$) δ 38.7 (37.0), 48.1, 49.1, 51.8, 52.7, 53.3, 54.1, 54.8, 55.7, 59.0, 65.3, 70.7, 71.7, 72.6, 72.8, 73.7, 74.4 (74.2), 75.1, 130.9, 131.3, 140.0, 172.0, 172.6, 175.1, 177.1.

**Gd·5a Complex (6a).** A suspension of **5a** (110 g, 0.184 mol) and $Gd_2O_3$ (31.4 g, 0.087 mol) was stirred at 50 °C, and the formation of the complex was monitored by HPLC and titration of the free ligand. When all oxide was consumed, further crops of $Gd_2O_3$ (6 × 300 mg, 0.005 mol) were added to the reaction mixture, without, however, resulting in an excess of free gadolinium ion. After 6 h, the formation of the complex was complete, the cloudy solution was filtered and evaporated to dryness, and the residue was dried in vacuo ($P_2O_5$; 14 mbar; 50 °C) to give **6a** (133.7 g; 97%) as a white solid: mp 233–235 °C.

**Gd·5b complex (6b)** was prepared from **5b** as reported for **6a** in 98% yield: mp 210 °C dec; $[\alpha]^{20}_D$ = +6.20° (*c* 5.018, MeOH).

**10-[2-[[2-Hydroxy-1-(hydroxymethyl)ethyl]amino]-1-(hydroxymethyl)-2-oxoethyl]-1,4,7,10-tetraazacyclododecane-1,4,7-triacetic Acid–Gd Complex (7a).** A solution of **6a** (75 g, 0.1 mol) in $H_2O$ (1.5 L) was subjected to hydrogenolysis at room temperature in the presence of 5% Pd/C (100 g). The reaction mixture was filtered, and the solvent was removed in vacuo to give **7a** as a white solid in quantitative yield: mp >280 °C.

**(*S*)-1-[[3-Hydroxy-2-[4,7,10-tris(carboxymethyl)-1,4,7,10-tetraazacyclododec-1-yl]-1-oxopropyl]methylamino]-1-deoxy-D-glucitol–Gd Complex (7b).** A solution of **6b** (66.8 g, 0.078 mol) in $H_2O$ (1 L) was subjected to hydrogenolysis at 50 °C in the presence of 5% Pd/C (75 g). The usual workup gave **7b** as a white solid: mp 204 °C dec; $[\alpha]^{20}_D$ = −12.8° (*c* 5.002, $H_2O$).

**X-ray Structure Analysis.** Single crystals of **6a** suitable for X-ray analysis were obtained by slow crystallization at 45 °C from a 1:1 (v/v) $H_2O$–DMSO solution. Investigation on a single crystal of **6a** was carried out with an Enraf-Nonius CAD4 X-ray automatic diffractometer. A summary of crystallographic data is reported in Table I. Unit cell parameters were determined by least-squares refinement of diffractometer setting angles of 25 carefully centered reflections. During data collection, three standard reflections were monitored periodically as a check of the diffractometer and of the crystal. Intensities were corrected for Lorentz and polarization effects. The data set was empirically corrected for absorption effects after the structure had been solved.[12] All calculations were performed on an IBM Personal System/2 Model 80 computer with the SHELX-76 set of programs[13] that uses the analytical approximation for the atomic scattering factors and anomalous dispersion corrections for all the atoms from ref 14. The molecular plots were produced by the program ORTEP.[15] The structure was solved by the heavy-atom technique, with the use of a Patterson map. Refinement was performed by means of the full-matrix least-squares method. The function minimized was $\sum w(|F_o| - |F_c|)^2$, with $w = 1/\sigma^2(F)$. Isotropic thermal parameters were used for the carbon atoms. Gadolinium, nitrogen, and oxygen atoms were refined anisotropically. Hydrogen atoms were introduced in calculated positions with an overall temperature factor $U$ of 0.05 Å$^2$. Some degree of disorder was found in the phenyl ring: two positions for the carbon atoms C16, C19, C20, and C21 were found, and population parameters of 0.7 and 0.3 were assigned to the different positions.

**Table I.** Crystallographic Data for $[(C_{27}H_{40}N_5O_{10})Gd\cdot H_2O]\cdot 3H_2O$

| | | | |
|---|---|---|---|
| mol formula | $C_{27}H_{48}N_5GdO_{14}$ | $\mu$, cm$^{-1}$ | 20.03 |
| mol wt | 823.95 | $D$, g cm$^{-3}$ | 1.69 |
| space group | $P2_1/C$ | λ(Mo Kα graphite-monochromated radiation), Å | 0.7107 |
| $a$, Å | 17.378 (4) | | |
| $b$, Å | 8.283 (7) | | |
| $c$, Å | 22.813 (5) | no. of obsd reflecns | |
| β, deg | 100.33 (2) | $I > 3\sigma(I)$ | 4419 |
| $V$, Å$^3$ | 3230 (3) | no. of refined params | 305 |
| $Z$ | 4 | $R^a$ | 0.040 |
| $F$(000) | 1684 | $R_w{}^b$ | 0.036 |

$^a R = \sum||F_o| - |F_c||/\sum|F_o|$. $^b R_w = [\sum w(|F_o| - |F_c|)^2/\sum w(F_o)^2]^{1/2}$.

**Potentiometry and Stability Constant Determinations.** Potentiometric measurements were carried out at 25.0 ± 0.1 °C in solutions maintained at a constant ionic strength of 0.1 M with $N(CH_3)_4NO_3$.

The solution of the ligands (0.001 mM) was titrated against 0.2 M $N(CH_3)_4OH$. The pH of the solution was monitored with a Metrohm E 636 potentiometer that was equipped with a 1-mL piston buret, a glass electrode, and a calomel reference electrode (KCl sat).

The stability constants of the gadolinium complexes were determined by using the competition reaction between **5a,b** ligands and the Gd–DTPA complex whose formation constant had been reported previously.[16] To overcome the problems associated with the slow kinetics, the solutions were heated to and maintained at 60 °C for 24 h; the pH of the solutions was measured after the sample was reconditioned at 25 °C for 48 h.[17] Equilibrium was considered to be reached when two successive pH measurements differed by less than 0.005 unit. The chemical integrity of the reactants was checked by HPLC after the last measurement.

The ligand protonation constants and $Gd^{3+}$ stability constants were obtained from the raw data by using SUPERQUAD.[18]

**NMR Measurements.** Water proton relaxation measurements (39 °C, 20 MHz) were carried out on a Minispec pc 120-Bruker on five solutions (0.2–5.0 mM) of the Gd chelate prepared from a 0.01 M stock solution by dilution with 0.15 M NaCl, pH 7.4. Spin–lattice relaxation times $T_1$ were measured by means of the inversion-recovery method, and spin–spin relaxation times $T_2$, by means of the Carr–Purcell–Meiboom–Gill (CPMG) pulse sequence.[19]

The $1/T_1$ NMRD profiles[20] of water protons were measured over a continuum of magnetic fields from $2.5 \times 10^{-4}$ to 1.4 T (corresponding to 0.01–50-MHz proton Larmor frequencies) on the Koenig–Brown relaxometer installed at the Department of Chemistry of the University of Florence (Italy).

The spectrometer works under complete computer control with an absolute uncertainty of $1/T_1$ of ±1%.

The experimental data were fitted by the Solomon–Bloembergen–Morgan equations, using $r$, $\tau_R$, $\tau_{SO}$, and $\tau_v$ as adjustable parameters.

## Results and Discussion

**Synthesis.** The general route followed for the preparation of complexes **6a,b** and **7a,b** is sketched in Scheme I.

Optical resolution of 2-chloro-3-(phenylmethoxy)propanoic acid (**1**) was achieved using (*R*)- and (*S*)-1-(phenylethyl)amine. (*R*)-**1**

(12) Walker, N.; Stuart, D. D. *Acta Crystallogr., Sect. A* **1983**, *39*, 158.
(13) Sheldrick, G. M. SHELX-76, Program for Crystal Structure Determination. University of Cambridge, England, 1976.
(14) *International Tables for X-ray Crystallography*; Kynoch: Birmingham, England, 1974; Vol. IV.
(15) Johnson, C. K. ORTEP; Report ORNL-3794; Oak Ridge National Laboratory: Oak Ridge, TN, 1971.
(16) (a) Harder, R.; Chaberek, S. J. *J. Inorg. Nucl. Chem.* **1959**, *11*, 197. (b) Moeller, T.; Thompson, L. C. *Ibid.* **1962**, *24*, 499.
(17) Cacheris, W. P.; Nickle, S. K.; Sherry, A. D. *Inorg. Chem.* **1987**, *26*, 958.
(18) Gans, P.; Sabatini, A.; Vacca, A. *J. Chem. Soc., Dalton Trans.* **1985**, 1195.
(19) Martin, M. L.; Delpuech, J. J.; Martin, G. J. *Practical NMR Spectroscopy*; Heyden: 1980.
(20) Koenig, S. H.; Brown, R. D., III. In *N.M.R. Spectroscopy of Cells and Organisms*; Gupta, R. K., Ed.; CRC Press: Boca Raton, FL, 1987; Vol. II, p 75.

**Table II.** Water Proton Relaxivities at 20 MHz, 39 °C, NaCl 0.15 M, pH = 7.3

| complex | $r_1$, $(mM \cdot s)^{-1}$ | $r_2$, $(mM \cdot s)^{-1}$ |
|---|---|---|
| Gd-DOTA | 3.56 (1) | 4.75 (3) |
| **6a** | 4.49 (1) | 5.99 (1) |
| **7a** | 4.03 (1) | 5.35 (1) |
| **6b** | 5.19 (1) | 7.29 (5) |
| **7b** | 4.33 (1) | 6.36 (5) |

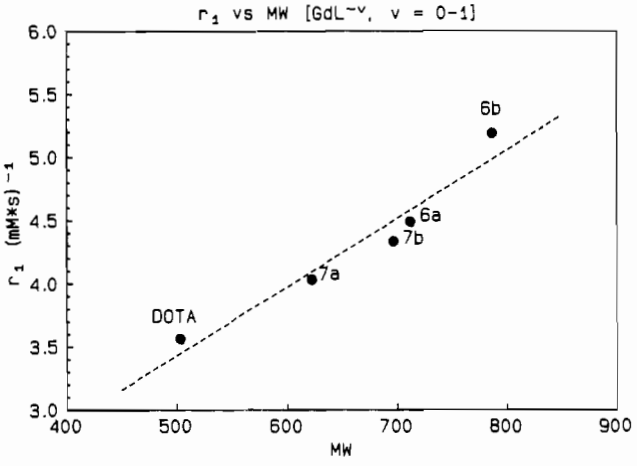


**Figure 1.** Plot of the longitudinal relaxivity measured at 20 MHz and 37 °C of Gd(III) chelates as a function of the molecular weight.

and (*S*)-**1**, with optical purities >98%, were recovered from the corresponding (*R*,*R*)- and (*S*,*S*)-(phenylethyl)ammonium salts, respectively. The configuration of (*R*)-**1** was assigned after reaction with aqueous ammonia and comparison of the *O*-benzylserine thus obtained with an analytical standard sample of (*S*)-*O*-benzylserine. The amides **3a,b** were prepared from **1** and (*R*)-**1** by classical chlorination with $SOCl_2$ followed by reaction in THF of acyl chlorides **2a,b** with 2-amino-1,3-propanediol and D-*N*-methylglucamine, respectively. Alkylation of 1,4,7,10-tetraazacyclododecane with **3a** in DMF at 50 °C gave **4a** in 47% yield (Scheme I). These or similar conditions could not be employed for the preparation of **4b** due to partial racemization of **3b** in DMF at 50 °C. Solvents such as DMSO, dimethylacetamide, and dioxane did not show a notable improvement. Eventually, reaction between 1,4,7,10-tetraazacyclododecane and **3b** without any solvent at controlled temperatures (80–90 °C) gave optically pure **4b** in 46% yield. Further alkylation of **4a,b** with sodium bromoacetate in $H_2O$ at pH 10 gave **5a** and **5b** in 82 and 45% yields, respectively. Complexation of ligands **5a,b** with $Gd_2O_3$ in $H_2O$ at 50 °C yielded the complexes **6a,b**. Hydrogenolysis of **6a,b** in $H_2O$ in the presence of Pd/C afforded debenzylated gadolinium complexes **7a,b**.

**Relaxivity Data.** The longitudinal and transverse water proton relaxivities of the complexes **6a,b** and **7a,b** at 39 °C and 20 MHz (Table II) show a very good correlation with their molecular weights (Figure 1). This behavior may be interpreted in terms of the dominant effect of the molecular reorientational time $\tau_R$. Furthermore, it supports the view that only one water molecule is present in the inner coordination sphere of these complexes, as was previously found for the parent Gd–DOTA complex. If more water molecules had been coordinated to the paramagnetic center, a dramatic increase in the observed relaxivity would have been found. Hence, the relaxivity value may represent a direct analytical tool to determine the number of coordinate water molecules in a series of structurally related complexes.

**Protonation and Stability Constant.** Table IIIa presents the protonation constants of DOTA and ligands **5a,b** as measured at 25 °C and $\mu$ = 0.1 M [$N(CH_3)_4NO_3$]; for comparative purposes, the values previously established for DOTA[21] and DOTA–PA[22]

**Table III**

a. Protonation Constants[a]

| reaction | log $K_{H_iL}$ DOTA[b] | **5a** | **5b** | DOTA–PA[c] |
|---|---|---|---|---|
| $L + H \rightarrow HL$ | 12.12 | 11.91 | 11.87 | 9.6 |
| $HL + H \rightarrow H_2L$ | 9.67 | 9.04 | 8.91 | 9.2 |
| $H_2L + H \rightarrow H_3L$ | 4.55 | 4.55 | 4.62 | 4.4 |
| $H_3L + H \rightarrow H_4L$ | 4.14 | | | |

b. Formation Constants of GdL Complexes[a]

| L | log $K_{GdL}$ |
|---|---|
| DOTA | 27.0 |
| | 28.0[d] |
| | 24.6[e] |
| **5a** | 25.9 |
| **5b** | 26.4 |

[a] At 25.0 °C; $\mu$ = 0.1 M, $N(CH_3)_4NO_3$. [b] From ref 23. [c] From ref 22. [d] From ref 24. [e] From ref 17.

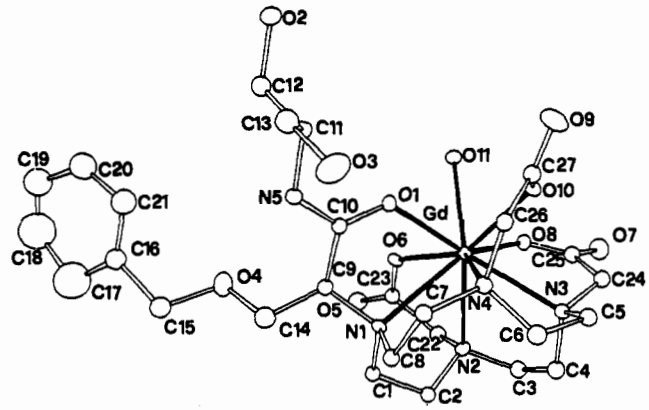


**Figure 2.** ORTEP drawing of the complex **6a**. For clarity, only one position for the atoms of the phenyl ring has been reported. The high thermal parameters of $C_{17}$ and $C_{18}$ are the consequence of the impossibility to distinguish their too much close disordered positions.

ligands are also reported. Our results for DOTA agreed well with those found by Delgado et al.,[23] which are higher than the values obtained by Desreaux.[21] This discrepancy may arise from the fact that the Desreaux measurements were performed in the presence of $Na^+$ ions; it is well-known that these macrocyclic ligands are able to significantly coordinate alkaline ions. For this reason, we carried out our titrations in the presence of tetramethylammonium ions.

We believe that the first protonation constant reported for DOTA–PA ligand suffers from the competition with $Na^+$ ions as well and therefore represents an underestimate when compared with the values found for **6a** and **6b** by our method.

The potentiometric determination of the formation constants of these Gd complexes is difficult due to both their extremely high value (log $K_{ML} \gg 20$) and the slow kinetics which characterize the formation of the complexes. This led us to determine the $K_{ML}$ value of a given complex through its competition reaction with DTPA–Gd (whose $K_{ML}$ had previously been reported), whereas the kinetic problems were solved by allowing the reaction mixture to reach the equilibrium conditions at 60 °C before taking the measurements at 25 °C.

Comparison between the $K_{ML}$ values for the Gd complex of DOTA and **6a,b** (Table IIIb) clearly indicates that the latter have maintained the strong complexing properties of the parent DOTA. We can assume that they act as octadentate ligands which wrap around the metal ion to form a tightly packed complex.

In order to verify this hypothesis and to assess the coordination properties of the amido group (as compared to the carboxylate

(21) Desreaux, J. F.; Merciny, E.; Loncin, M. F. *Inorg. Chem.* **1981**, *20*, 987.
(22) Sherry, A. D.; Brown, R. D.; Geraldes, C. F. G. C.; Koenig, S. H.; Kuan, K.-T.; Spiller, M. *Inorg. Chem.* **1989**, *28*, 620.
(23) Delgado, R.; Frausto da Silva, J. J. R. *Talanta* **1982**, *29*, 815.
(24) Desreaux, J. F. *Bull. Cl. Sci., Acad. R. Belg.* **1979**, *64*, 814.

**Table IV.** Positional Parameters ($\times 10^4$) and $U_{eq}$ or $U_{iso}$ ($\times 10^3$) for $[(C_{27}H_{40}N_5O_{10})Gd\cdot H_2O]\cdot 3H_2O$ (Esd in Parentheses)

| atom | x/a | y/b | z/c | $U_{eq/iso}$, Å$^2$ |
|---|---|---|---|---|
| Gd | 7819 (1) | 3046 (1) | 2579 (1) | 22 (1) |
| N1 | 6905 (3) | 3299 (9) | 1483 (3) | 26 (4) |
| N2 | 6354 (4) | 3732 (9) | 2644 (3) | 33 (4) |
| N3 | 7691 (4) | 5864 (9) | 3081 (3) | 31 (4) |
| N4 | 8237 (4) | 5504 (8) | 1914 (3) | 29 (4) |
| N5 | 8328 (3) | 1146 (9) | 819 (3) | 32 (4) |
| O1 | 8355 (3) | 1916 (8) | 1775 (2) | 31 (3) |
| O2 | 10118 (3) | −1378 (8) | 987 (3) | 47 (4) |
| O3 | 9394 (4) | 3501 (8) | 524 (3) | 75 (5) |
| O4 | 6641 (4) | −103 (9) | 440 (3) | 66 (5) |
| O5 | 5822 (3) | −415 (3) | 2392 (3) | 51 (4) |
| O6 | 6985 (3) | 777 (7) | 2430 (2) | 31 (3) |
| O7 | 7855 (4) | 3888 (9) | 4503 (3) | 60 (5) |
| O8 | 7770 (3) | 2841 (7) | 3593 (2) | 33 (3) |
| O9 | 10249 (3) | 4651 (8) | 2651 (3) | 55 (4) |
| O10 | 9106 (3) | 4056 (7) | 2904 (2) | 32 (3) |
| O11 | 8672 (3) | 813 (7) | 2954 (2) | 32 (3) |
| O12 | 9372 (4) | 547 (9) | 4174 (3) | 80 (5) |
| O13 | 4297 (6) | 3145 (12) | 3702 (4) | 134 (8) |
| O14 | 8287 (6) | 383 (13) | 4794 (5) | 243 (9) |
| C1 | 6055 (4) | 3275 (11) | 1539 (3) | 29 (2) |
| C2 | 5899 (5) | 4279 (11) | 2048 (3) | 32 (2) |
| C3 | 6302 (5) | 4990 (11) | 3104 94) | 38 (2) |
| C4 | 6866 (5) | 6374 (11) | 3033 (4) | 42 (2) |
| C5 | 8124 (4) | 7159 (11) | 2817 (3) | 35 (2) |
| C26 | 7972 (5) | 7062 (12) | 2140 (3) | 40 (2) |
| C7 | 7895 (4) | 5355 (11) | 1266 (4) | 32 (2) |
| C8 | 7046 (5) | 4838 (10) | 1175 (4) | 32 (2) |
| C9 | 7102 (4) | 1822 (12) | 1167 (3) | 31 (2) |
| C10 | 7990 (4) | 1648 (10) | 1263 (4) | 28 (2) |
| C11 | 9150 (5) | 843 (10) | 906 (4) | 32 (2) |
| C12 | 9201 (5) | −956 (11) | 854 (4) | 39 (2) |
| C13 | 9531 (5) | 1790 (12) | 465 (4) | 49 (3) |
| C14 | 6674 (5) | 1601 (12) | 541 (4) | 48 (3) |
| C15 | 6232 (6) | −508 (14) | −158 (5) | 68 (3) |
| C16[a] | 6486 (8) | −2245 (17) | −325 (6) | 49 (4) |
| C161[b] | 5977 (14) | −2402 (31) | −141 (11) | 45 (6) |
| C17 | 5945 (8) | −3023 (22) | −653 (7) | 170 (5) |
| C18 | 6196 (9) | −4760 (21) | −744 (7) | 158 (5) |
| C19[a] | 6624 (11) | −5187 (22) | −654 (8) | 86 (5) |
| C191[b] | 5716 (14) | −5480 (32) | −487 (11) | 46 (6) |
| C20[a] | 7335 (10) | −4182 (23) | −342 (7) | 77 (5) |
| C201[b] | 5275 (15) | −4768 (36) | −172 (12) | 41 (7) |
| C21[a] | 7210 (9) | −2701 (20) | −171 (7) | 67 (4) |
| C211[b] | 5402 (12) | −3168 (30) | −8 (9) | 32 (5) |
| C22 | 6005 (5) | 2207 (11) | 2828 (4) | 39 (2) |
| C23 | 6287 (5) | 707 (12) | 2528 (4) | 36 (2) |
| C24 | 8038 (5) | 5660 (11) | 3717 (4) | 37 (2) |
| C25 | 7874 (5) | 3989 (12) | 3954 (4) | 39 (2) |
| C256 | 9116 (4) | 5452 (11) | 1983 (4) | 33 (2) |
| C27 | 9513 (5) | 4669 (11) | 2545 (4) | 34 (2) |

[a] Occupation factor: 0.7. [b] Occupation factor: 0.3.

functionalities), we determined the X-ray structure of **6a**.

**Description of the Structure of 6a.** The structure consists of a $Gd(C_{27}H_{40}N_5O_{10})(H_2O)$ unit and three water molecules. Positional parameters for non-hydrogen atoms and selected bond distances and angles are reported in Tables IV and V. The gadolinium ion shows a nine-coordinate stereochemistry with coordinating sites occupied by the four amine nitrogens N(1), N(2), N(3), and N(4), three carboxylate oxygens O(6), O(8), and O(10), one carboxamide oxygen O(1), and one water oxygen O(11) (Figure 2).

The coordination polyhedron can be described as a distorted-square antiprism capped with the coordinated water oxygen in the axial position, as shown in Figure 3. All Gd–O distances, ranging from 2.34 to 2.43 Å, are very similar and unambiguously show the participation of the carboxamide oxygen in the complexation of gadolinium. As expected, Gd–O distances ($Gd-O_{av}$ 2.37 Å) are significantly shorter than those observed for the Gd–N bonds ($Gd-N_{av}$ 2.67 Å). The coordinated water oxygen is at 2.43 Å from the gadolinium atom, and this value is comparable with metal–$H_2O$ distances observed in other complexes of lanthanides

**Table V.** Selected Bond Distances (Å) and Angles (deg) for $[(C_{27}H_{40}N_5O_{10})Gd\cdot H_2O]\cdot 3H_2O$ (Esd in Parentheses)

| | | | |
|---|---|---|---|
| **Bond Distances** | | | |
| Gd–N1 | 2.719 (6) | Gd–O1 | 2.392 (6) |
| Gd–N2 | 2.638 (7) | Gd–O6 | 2.360 (5) |
| Gd–N3 | 2.627 (7) | Gd–O8 | 2.337 (5) |
| Gd–N4 | 2.714 (7) | Gd–O10 | 2.378 (5) |
| | | Gd–O11 | 2.429 (5) |
| **Bond Angles** | | | |
| O10–Gd–O11 | 71.2 (2) | N3–Gd–O6 | 132.3 (2) |
| O8–Gd–O11 | 74.0 (2) | N3–Gd–O1 | 139.2 (2) |
| O8–Gd–O10 | 85.2 (2) | N3–Gd–N4 | 68.2 (2) |
| O6–Gd–O11 | 76.4 (2) | N2–Gd–O11 | 132.7 (2) |
| O6–Gd–O10 | 147.5 (2) | N2–Gd–O10 | 140.3 (2) |
| O6–Gd–O8 | 87.4 (2) | N2–Gd–O8 | 75.7 (2) |
| O1–Gd–O11 | 71.0 (2) | N2–Gd–O6 | 66.8 (2) |
| O1–Gd–O10 | 84.4 (2) | N2–Gd–O1 | 129.8 (2) |
| O1–Gd–O8 | 145.0 (2) | N2–Gd–N4 | 103.2 (2) |
| O1–Gd–O6 | 63.8 (2) | N2–Gd–N3 | 68.1 (2) |
| N4–Gd–O1 | 124.1 (2) | N1–Gd–O11 | 127.0 (2) |
| N4–Gd–O10 | 65.1 (2) | N1–Gd–O10 | 128.4 (2) |
| N4–Gd–O8 | 132.0 (2) | N1–Gd–O8 | 142.9 92) |
| N4–Gd–O6 | 137.3 (2) | N1–Gd–O6 | 71.7 (2) |
| N4–Gd–O1 | 71.6 (2) | N1–Gd–O1 | 64.5 (2) |
| N3–Gd–O11 | 128.1 (2) | N1–Gd–N4 | 66.4 (2) |
| N3–Gd–O10 | 72.5 (2) | N1–Gd–N3 | 104.6 (2) |
| N3–Gd–O8 | 67.2 (2) | N1–Gd–N2 | 68.0 (2) |

**Table VI.** Primary Coordination Sphere Distances (Å) for Gadolinium Polyamino Polycarboxylate Complexes

| | 6a | Gd–DOTA[a] | Gd–DTPA[b] | Gd–(DTPA–BEA)[c] |
|---|---|---|---|---|
| metal–$N_{av}$ | 2.67 | 2.66 | 2.64 | 2.70 |
| metal–$O_{av}$ | 2.37 | 2.36 | 2.41 | 2.37 |
| metal–$O_{water}$ | 2.43 | 2.46 | 2.49 | 2.42 |

[a] From ref 25. [b] From ref 6. [c] From ref 26.

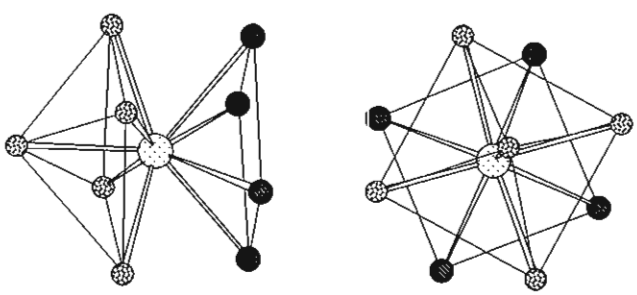

**Figure 3.** Coordination polyhedron formed by the ligand atoms about the Gd(III) ion.

with polyamino polycarboxylic ligands containing water molecules in the first coordination sphere of the metal.

The four nitrogen atoms of the macrocycle and the oxygen donor atoms involved in the complexation of the gadolinium lie in two mean planes, and the displacement of these atoms from their respective least-squares planes is <0.02 and <0.03 Å, respectively. The two planes are parallel within 0.5°, and the gadolinium ion lies 1.65 and 0.68 Å from the plane of the nitrogen atoms and that of the oxygen atoms, respectively. The coordinated water oxygen is 1.74 Å from the O1–O6–O8–O10 mean plane, with the $Gd-O_{water}$ bond nearly perpendicular to the mean plan described by the oxygen donor atoms ($\alpha = 3.2°$). The coordinated water molecule (O11) and the other two molecules of the crystal lattice (O12, O14) (see Figure 4) form a close hydrogen bond pattern, which ends at the oxygen O7. Furthermore, two different molecules, related by a glide plane, are connected by the water molecule O14 which forms hydrogen bonds with the carboxylic oxygen O7 and the alcoholic oxygen O3. Finally, the oxygen atoms O4 and O5 of each molecule are joined by the fourth water molecule O13. This arrangement accounts for the high hydrophilicity of this species and nicely visualizes the various interactions involving the outer-sphere water molecules at the surface of the

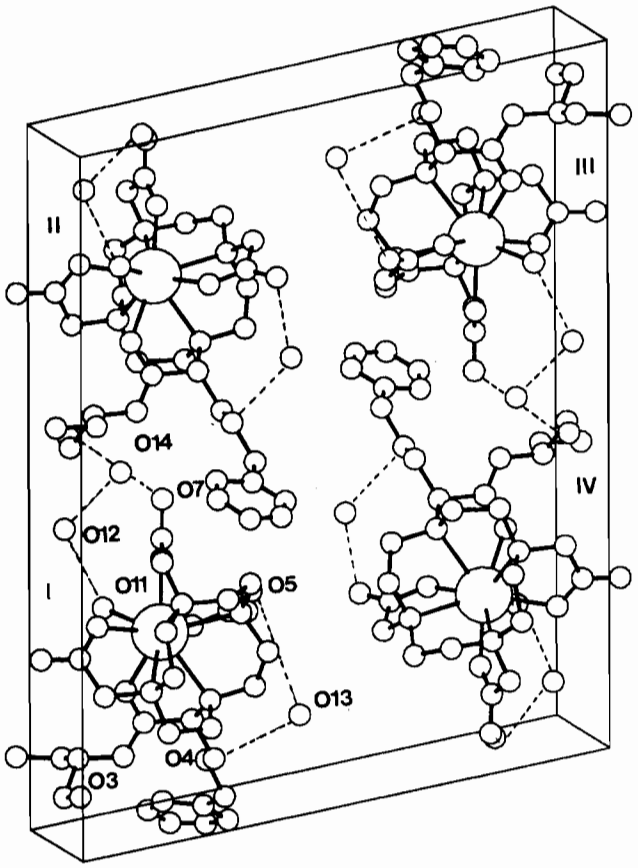


**Figure 4.** Perspective view of the solid-state structure of **6a** including the coordinated water molecule (011) and the other two water molecules (012, 014) of the crystal lattice.

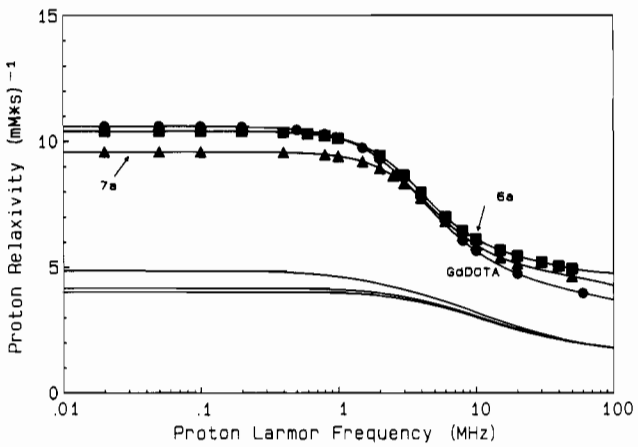


**Figure 5.** $1/T_1$ NMRD profiles of 1 mM aqueous solutions of Gd–DOTA (●), **7a** (▲), and **6a** (■), measured at 25 °C and pH = 7.3. The solid curves through the experimental data are calculated with the parameters of Table VII and are the sum of the inner- and outer-sphere contributions. The latter was calculated by using Freed's equation, assuming a value of 3.6 Å for the distance of the closest approach of the Gd(III) complex and water molecules and a value of $2.6 \times 10^{-5}$ cm$^2$ s$^{-1}$ for their relative diffusion constant.

complex. Comparison of the solid-state structure of **6a** with that of the Gd(DOTA)($H_2O$)[25] complex reveals many similarities. The coordination environments around the metals are very similar, and the average metal–O, metal–N, and metal–$O_{water}$ distances are identical within 0.05 Å (see Table VI). Very recently, the crystal structure of the gadolinium complex of DTPA bis(amide), Gd(DTPA–BEA)($H_2O$), has been reported[26] showing for the first

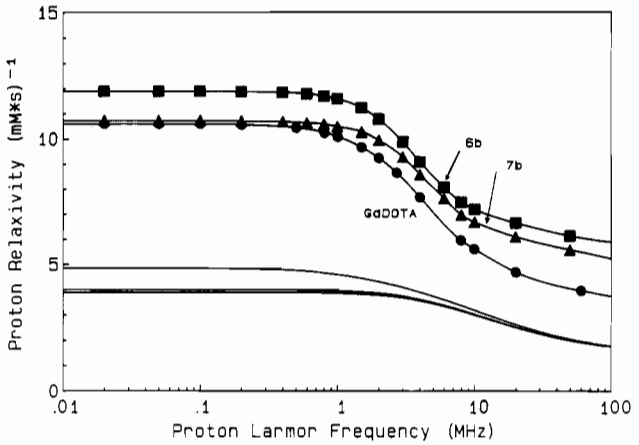


**Figure 6.** $1/T_1$ NMRD profile of 1 mM aqueous solutions of Gd–DOTA (●), **7b** (▲), and **6b** (■), measured at 25 °C and pH = 7.3. The best-fit curves are calculated as described in the caption to Figure 5.

**Table VII.** NMR Parameters Obtained from the Fitting of NMRD Profiles with the Inner-Sphere Relaxation Theory[2]

| complex | $\tau_{SO}$, ps | $\tau_V$, ps | $\tau_R$, ps | $r$, Å |
|---|---|---|---|---|
| Gd–DOTA | 458 | 26 | 72 | 3.10 |
| **7a** | 142 | 21 | 81 | 3.08 |
| **6a** | 137 | 16 | 92 | 3.02 |
| **7b** | 122 | 25 | 96 | 3.00 |
| **6b** | 140 | 25 | 123 | 3.00 |

time that carboxamide oxygens may be directly involved in the complexation of gadolinium. For this complex, the coordination polyhedron is described as a tricapped trigonal prism. Nevertheless, the average Gd–O and Gd–N distances are very similar to those found for **6a**.

**Relaxation Studies.** The $1/T_1$ NMRD profiles of the aqueous solutions of Gd–DOTA, **6a,b**, and **7a,b** (Figures 5 and 6) were set up in order to establish the effects caused by the amide functionalities on the parameters that determine the observed relaxivities.

As we reported above, at 20 MHz a linear correlation is found between the observed relaxivities $r_1$ and the molecular weights (Figure 1) due to the dominant contribution of the rotational tumbling time $\tau_R$, which clearly reflects—in these closely related species—the changes in their molecular size. This distinct relationship further indicates that the number of coordinated water molecules ($q$) in the inner coordination sphere of the Gd(III) ion is 1, which is identical to the findings in the X-ray structure of **6a** and the results of the $1/T_1$ NMRD measurement on an aqueous solution of the DOTA–Gd complex. However, this linear dependence of $r_1$ on $\tau_R$ is readily lost as the observation frequency decreases: **6a** reaches the relaxivity of DOTA–Gd at 1 MHz, and **7a**, at 4 MHz. The observed behavior parallels the findings reported for DOTA–PA–Gd[22] and reflects the increased contribution of the electronic relaxation time to the correlation time $\tau_c$ as the observation frequency decreases. Complex **6b** has a higher relaxivity than DOTA–Gd at any field owing to a much longer $\tau_R$ which can counterbalance (at least in part) the short $\tau_s$ value at low fields.

Table VII shows that the values found for $\tau_{SO}$ in the whole series are almost independent of the nature of the amide substituents. A very similar value for $\tau_{SO}$ (132 ps) was found by Koenig et al. in the analysis of the $1/T_1$ NMRD profile of the DOTA–PA–Gd complex. This supports the hypothesis that the marked decrease in $\tau_{SO}$, which was observed to pass from the highly symmetric DOTA to its substituted amide derivatives, is mainly related to the amide group itself. On the other hand, on considering a related series of DOTA derivatives with substituents at the methylene acetate carbons, we noted[27] that only a minor decrease in $\tau_{SO}$ was

(25) Contrast and Contrast Agents in Magnetic Resonance Imaging. A Special Topic Seminar Trondheim, Norway, 12–13 September, 1988. Rinck, Peter A., Ed.

(26) Konings, M. S.; Dow, W. C.; Love, D. B.; Raymond, K. N.; Quay, S. C. *Inorg. Chem.* **1990**, *29*, 1488.

**Scheme I**

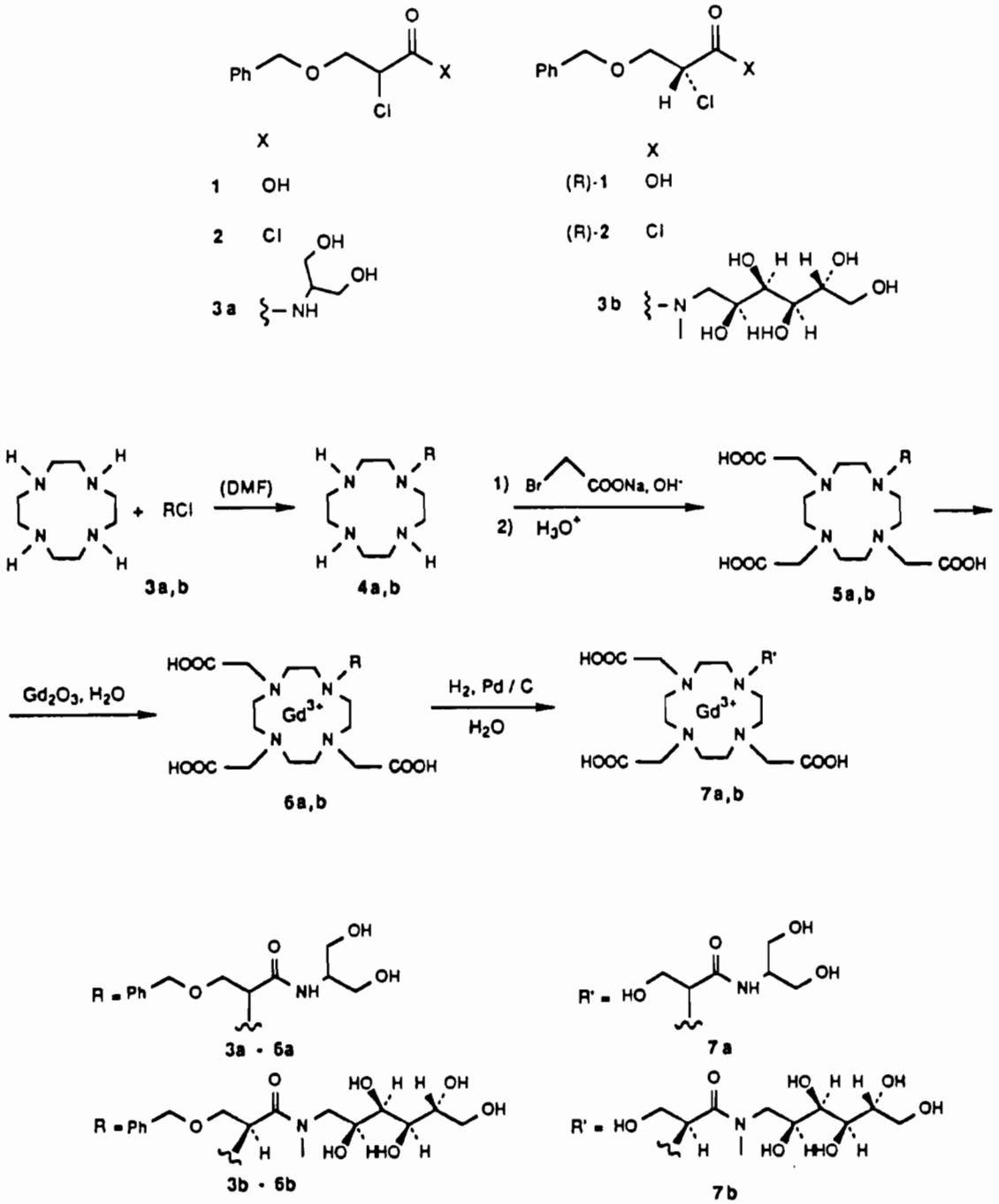


due to the substitution. It is likely that the observed decrease in $\tau_{SO}$ depends on the decreased donor ability of the amide oxygen with respect to the carboxylate oxygen. Therefore, the $\tau_{SO}$ parameter acts as a molecular amplifier of the minor difference in the coordination of carboxylate vs amide groups.

## Conclusions

Our results may be summarized as follows: (a) The transformation of a carboxylate into an amide group does not alter the coordination capabilities of these macrocyclic ligands, as evidenced by the high formation constants of the **6a,b** complexes. (b) The X-ray structure of **6a** shows that, inside the square antiprismatic coordination cage, the Gd–O bond distances are quite similar, irrespective of the nature of the donor (carboxylate or carboxamide group). (c) The analysis of the $1/T_1$ NMRD profiles reveals that the main change induced by the carboxylate → amide transformation is a drastic reduction of $\tau_{SO}$, which in turn is responsible for a decreased relaxivity at low fields. At the imaging frequencies (e.g., 20 MHz), the relaxivity observed is linearly related to the molecular size. In conclusion, these findings may contribute significantly to the design of new powerful MRI contrast agents.

**Registry No.** **1**, 113786-49-5; (*R*)-**1**, 139542-64-6; (*S*)-**1**, 139542-63-5; **2**, 124628-32-6; (*R*)-**2**, 140697-12-7; **3a**, 124628-33-7; **3b**, 140697-13-8; **4a**, 124628-14-4; **4b**, 140697-14-9; **5a**, 124628-24-6; **5b**, 140833-98-3; **6a**, 140697-07-0; **6a**·3$H_2O$, 140697-11-6; **6b**, 140697-08-1; **7a**, 140697-09-2; **7b**, 140697-10-5; Gd·DOTA, 72573-82-1; 2-amino-1,3-propanediol, 534-03-2; D-*N*-methylglucamine, 6284-40-8; 1,4,7,10-tetraazacyclododecane, 294-90-6.

**Supplementary Material Available:** Listings of positional parameters for non-hydrogen atoms (Table S1), anisotropic and isotropic thermal parameters (Table S2), positional parameters for the hydrogen atoms (Table S3), and complete bond distances and angles (Table S4) (6 pages); a listing of observed and calculated structure factors (21 pages). Ordering information is given on any current masthead page.

(27) Aime, S.; Botta, M.; Ermondi, G.; Fedeli, F.; Uggeri, F. *Inorg. Chem.* **1992**, *31*, 1100.